Front. Energy 2020, 14(4): 683–698
https://doi.org/10.1007/s11708-020-0705-0

RESEARCH ARTICLE

Jitan WU, Yonglin JU

Comprehensive comparison of small-scale natural gas liquefaction processes using brazed plate heat exchangers

Abstract The brazed plate heat exchanger (BPHE) has some advantages over the plate-fin heat exchanger (PFHE) when used in natural gas liquefaction processes, such as the convenient installation and transportation, as well as the high tolerance of carbon dioxide (CO_2) impurities. However, the BPHEs with only two channels cannot be applied directly in the conventional liquefaction processes which are designed for multi-stream heat exchangers. Therefore, the liquefaction processes using BPHEs are different from the conventional PFHE processes. In this paper, four different liquefaction processes using BPHEs are optimized and comprehensively compared under respective optimal conditions. The processes are compared with respect to energy consumption, economic performance, and robustness. The genetic algorithm (GA) is applied as the optimization method and the total revenue requirement (TRR) method is adopted in the economic analysis. The results show that the modified single mixed refrigerant (MSMR) process with part of the refrigerant flowing back to the compressor at low temperatures has the lowest specific energy consumption but the worst robustness of the four processes. The MSMR with fully utilization of cold capacity of the refrigerant shows a satisfying robustness and the best economic performance. The research in this paper is helpful for the application of BPHEs in natural gas liquefaction processes.

Keywords liquefied natural gas, brazed plate heat exchanger, energy consumption, economic performance, robustness

Received Jan. 17, 2019; accepted Mar. 19, 2020; online Nov. 10, 2020

Jitan WU, Yonglin JU (✉)
Institute of Refrigeration and Cryogenics, Shanghai Jiao Tong University, Shanghai 200240, China
E-mail: yju@sjtu.edu.cn

1 Introduction

Natural gas has been the fossil energy resource with the fastest growth recently as a relatively clean energy resource [1]. Liquefied natural gas (LNG) is widely used in many countries around the world primarily as a mode to transport natural gas [2]. With the worldwide application of natural gas, the LNG industry is booming since LNG has been an important solution for energy security in many countries where it is not economical to use pipeline transmission of natural gas [3]. Furthermore, LNG trade is forecasted to meet one-third the natural gas demand in the next three decades [4]. As a result, the research of the performance of the LNG process is drawing more and more attention and the equipment applied in the LNG process are also well studied by many research groups.

Nguyen et al. [5] recently compared three small-scale LNG systems based on energy and exergy assessment and found that the mixed refrigerant (MR) process is more efficient than the expander-based ones. Khan and Lee [6] optimized the single mixed refrigerant (SMR) process with the help of the particle swarm paradigm and successfully improved efficiency by reducing the compression energy requirement by 10% compared with the base case. He et al. [7] optimized and comprehensively compared MSMR and the parallel nitrogen expansion cycle (PNEC) and discovered that MSMR had a lower specific energy consumption, a higher exergy efficiency, a lower total investment, and a higher flexibility than PNEC. Mehrpooya and Ansarinasab [8] conducted a detailed exergoeconomic evaluation of three popular SMR processes. The results indicated that the most important elements in exergy destruction cost are from PFHEs while the exergoeconomic factor in compressors is higher than other elements. Qyyum et al. [9] managed to replace the Joule-Thompson (J-T) valves in the SMR process with hydraulic turbines. The replacement saved 16.5% of the required energy and increased the exergy efficiency by 11%. Tan et al. [10] proposed a new liquefaction process for boil-off gas (BOG) based on the dual mixed refrigerant

(DMR) cycle. The new system achieved a coefficient of performance (COP) of 0.25 and an exergy efficiency of 41.3%. Cao et al. [11] investigated the robustness of the SMR process. They discussed the heat exchange process and the exergy loss in the recuperative heat exchanger and found that the robustness of the mixed refrigerant composition was very strong even though the ratio of the mixed refrigerant was restrained. They also proposed a novel method for adjusting the mixed refrigerant to achieve a higher efficiency.

There are also many studies that focus on offshore natural gas liquefaction processes. Hwang et al. [12] proposes a generic liquefaction model to represent various types of liquefaction cycles based on the DMR cycle in liquefied natural gas floating, production, storage, and offloading (LNG-FPSO) applications. They developed 27 different cases from the generic model. The power required for the optimal case was decreased by 7.45% compared with that of the previous presented DMR cycle. They also formulated a mathematical model of the DMR cycle and obtained the optimal operation condition using a hybrid optimization method that consists of GA and sequential quadratic programming (SQP) [13]. The results showed that the required power was decreased by 34.5% compared with the patent and by 1.2% compared with that described in existing literature. Xiong et al. [14] proposed three pressurized liquefied natural gas (PLNG) processes for offshore application, including the cascade, the SMR, and the single expander PLNG processes. The processes were optimized by GA, which had an energy saving of 46%, 50%, and 63%, respectively, compared to the representative conventional LNG process. The PLNG processes also presented a smaller heat transfer area than the representative conventional LNG process.

All the researches mentioned above focused on the LNG processes based on the multi-stream heat transfer process using PFHEs. As the most important heat transfer equipment, the multi-stream PFHE is widely applied in small-scale LNG plants for high heat transfer efficiency. Massive studies have been reported on the performance of PFHEs and the LNG process using PFHEs. de Mello et al. [15] investigated the heat transfer, pressure drop, and structural characteristics of a ceramic PFHE by computational fluid dynamics (CFD) simulation and experimental test at a high temperature. Wang and Li [16] proposed a combined method to consider the surface selection and layer pattern optimization of the multi-stream PFHE simultaneously. The combined method improved the heat transfer performance and reduced the pressure drop to a large extent. Ma et al. [17] investigated the influence of the structure parameters on the stress of the plate-fin in a PFHE applied in the LNG process based on the finite element method (FEM) and the thermal elastic theory. They found that the peak value of the equivalent stress was at the brazed joint near the fin side and the peak value was obviously impacted by the brazing seam thickness, fin thickness, and fin distance. Zhan et al. [18] studied the dynamic performance of nitrogen expansion LNG process with a PFHE model simplified according to symmetric layer arrangements. The results of the simulation showed that the symmetric layer arrangements of the PFHEs can significantly simplify the general model and reduce the calculation load.

However, the PFHE has some disadvantages in practical engineering. For instance, the PFHE cold box must be installed vertically for a better heat transfer performance [19], which results in the inconvenience for engineering. Furthermore, the channels of the PFHE are very thin and geometrically complicated, which can be easily blocked by solid impurities so that the standard of pre-treatment must be very strict. In many countries the concentration of CO_2 at the inlet of the LNG cold box is limited to as low as 50 ppm [20]. As a result, the conventional LNG processes using PFHEs are usually equipped with enormous purification unit to remove the impurities with a high freezing point such as carbon dioxide (CO_2), which leads to expensive impurity removal cost.

BPHEs have been suggested to replace the PFHEs in small-scale LNG process in recent years to overcome such disadvantages [20]. On one hand, one PFHE can be transformed into several small BPHEs equivalently. Each single BPHE is still vertically installed but they can be connected horizontally so that the height of the cold box can be remarkably reduced. Therefore, the installation and transportation of the LNG cold box will be more convenient and economically beneficial, especially in small-scale LNG plants with skid mounted packages. On the other hand, the inner structure of the BPHE is simpler than that of the PFHE, which makes the BPHE less likely to be blocked by solid impurities. Previous experimental research indicated that the tolerance to the CO_2 impurity of the BPHE was much higher than that of the PFHE when the heat exchanger is used to liquefy the natural gas [21]. Therefore, applying BPHEs in the LNG process may substantially decline the requirement of impurity removal and save the cost of the pre-treatment system.

However, it is still a new concept to use BPHEs in LNG processes. Therefore, studies on the LNG processes using BPHEs is few and far between. He et al. [1] presented a detailed state-of-art review of the recent progress on the design and optimization of natural gas liquefaction processes for both onshore and offshore applications in which 99 papers are included. Almost all the mentioned studies focused on the LNG processes using multi-stream heat exchangers while none of them focused on the processes with BPHEs.

The BPHE with a high tolerance to CO_2 impurity only has two channels [21], one for the hot stream and the other for the cold stream. This is the main reason why the BPHEs cannot be applied directly in the existing LNG processes which are designed for multi-stream heat exchangers. A method [22] has previously been proposed to transform a conventional PFHE process into a BPHE process, as illustrated in Fig. 1. However, only one BPHE process has been proposed and analyzed by using this method so far. Massive studies are still needed to develop and analyze the LNG processes using BPHEs since the BPHE processes can be significantly different from the PFHE processes. As shown in Fig. 1, the cold stream cools the hot streams separately in the process using BPHEs. Although the inlet and outlet conditions of the streams can be defined to be the same as those of the original process using PFHE, the heat transfer procedure and the composite curves inside the heat exchangers can be very different. In a multi-stream heat exchanger, the heat can transfer freely through every channel, including the different hot sides. As a result, the heat can transfer from the hot sides with higher temperatures to the hot sides with the temperatures close to the temperature of the cold side at the pinch point. On the contrary, the hot sides are in isolated heat exchangers in the BPHE process so that the heat cannot transfer between different hot sides. It is more likely that the hot and cold composite curves get too close or even cross at the pinch point if the heat transfer procedure cannot be affected by a third stream. Therefore, the variable design of the BPHE process is much stricter than the original process using PFHEs although the structures of the processes seem similar.

In the present work, four mixed refrigerant cycle (MRC) processes using BPHEs are optimized and comprehensively compared in terms of energy consumption, economic performance, and robustness. Three of the processes are transformed from the PFHE processes which have been already presented by other research groups. The last one is a reported offshore BOG reliquefaction process using BPHEs.

2 Process description

Case 1 is transformed from the typical poly refrigerant integrated cycle operations (PRICO) process [23–25] first developed by Black and Veatch Pritchard, which is the most widely applied and studied SMR process. The conventional PRICO process and the modified PRICO process with BPHEs are illustrated in Figs. 2(a) and 2(b), respectively.

In Case 1, natural gas is first pressurized by a compressor (C-101) and cooled by a water cooler (WC-101). Then, it is liquefied in BPHE-1. After that, the LNG is throttled to depressurize for storage. The MR is first pressurized (C-102), cooled (WC-102), and then flows into a vapor-liquid separator (S-102). The vapor phase is pressurized and cooled again while the liquid phase is pumped to the same pressure. Next, the two phases are mixed and precooled in a heat exchanger (BPHE-2). The precooled refrigerant flows through a J-T valve (J-102). The temperature of the throttled refrigerant decreases. Then, it is divided into two streams which flow into different heat exchangers as the cold side to cool the warm refrigerant or liquefy the natural gas. Finally, the two streams converge and then flow back to the entrance of the compressor (C-102).

The advantage of the PRICO process is that the process is very simple so that fewer variables are monitored and fewer BPHEs are needed, which leads to a simple process design and convenient operation. Additionally, less equipment is required in the PRICO process compared with other processes so that the investment in equipment purchase can be very low.

Case 2 is transformed from a popular MSMR process developed by He and Ju [26]. The mixed refrigerant is separated into the vapor phase and the liquid phase. Then, the two phases enter the cold box separately. The original process and the modified process using BPHEs are demonstrated in Figs. 3(a) and 3(b), respectively.

In Case 2, natural gas is also pressurized in a compressor (C-101) and cooled in a water cooler (WC-101) first. Then, the natural gas flows through two BPHEs, one for precooling (BPHE-1) and the other for liquefaction

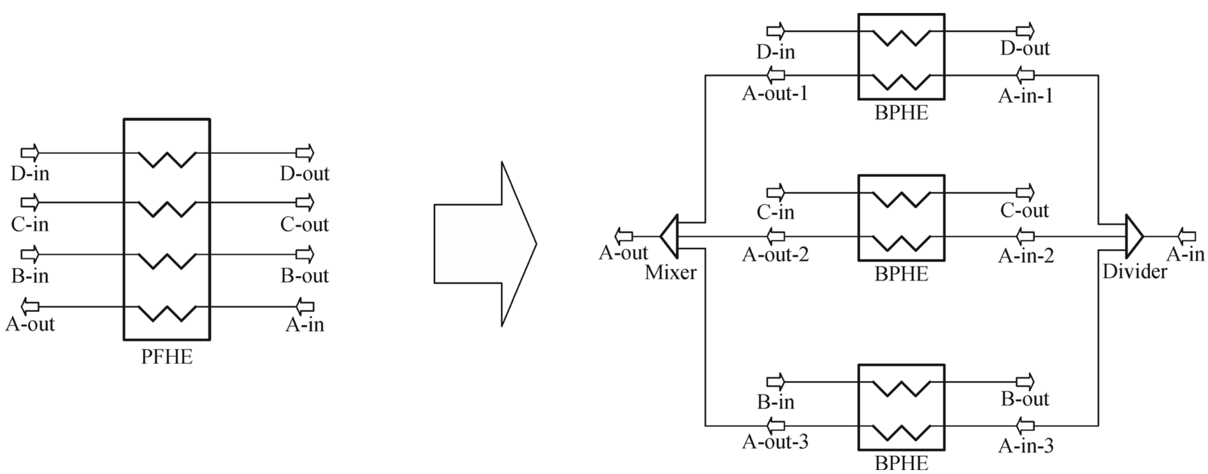

Fig. 1 Method of process transformation (adapted with permission from Ref. [22]).

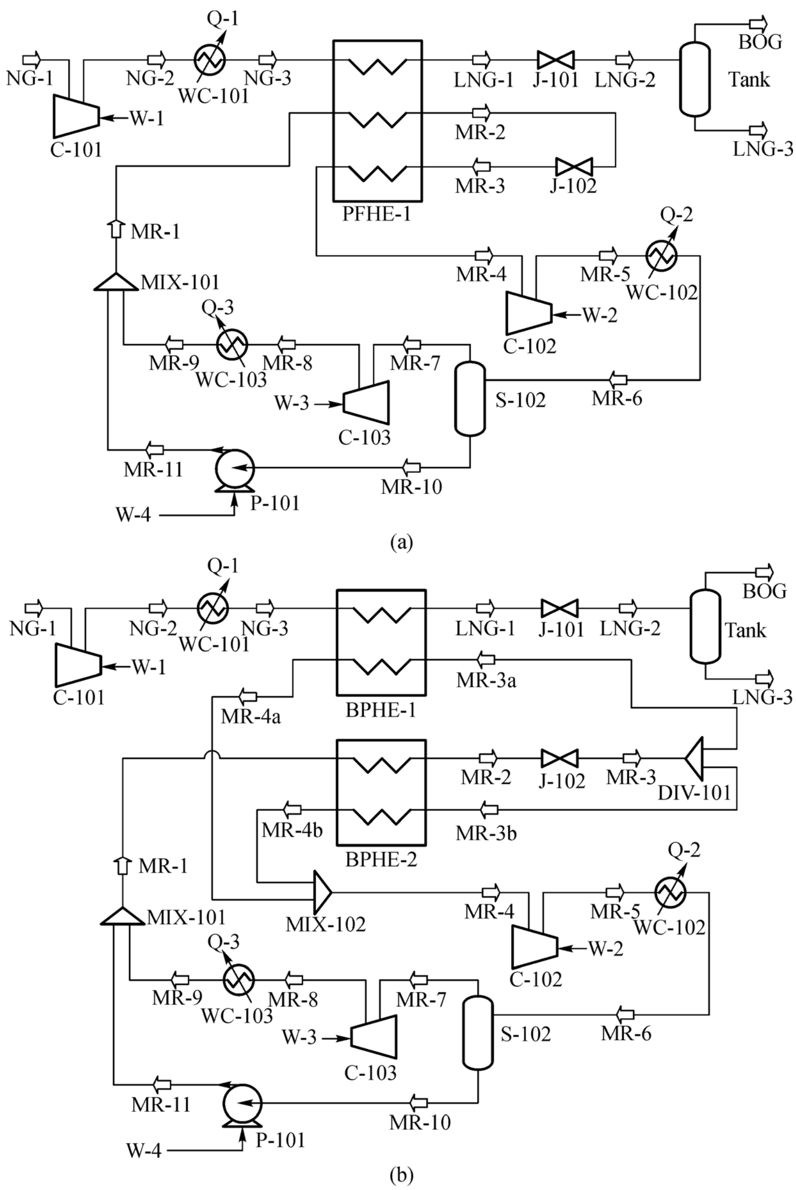

Fig. 2 Conventional PRICO process and modified PRICO process with BPHEs.
(a) Conventional PRICO process; (b) modified PRICO process with BPHEs (Case 1).

(BPHE-4). The LNG is also throttled and then flows into the LNG tank. The MR is first pressurized and cooled in two stages (C-102 and C-103). Then, the refrigerant enters a vapor-liquid separator (S-102). The vapor phase and the liquid phase enter the cold box separately. The vapor phase (MR-10) is cooled in a precooling BPHE (BPHE-2) and liquefied in a subcooling BPHE (BPHE-5). Then, it is throttled to a lower pressure and temperature and divided into two streams, one flowing back to the subcooling BPHE (BPHE-5) to liquefy the vapor refrigerant and the other to the liquefaction BPHE (BPHE-4) to liquefy the natural gas as the cold side. Meanwhile, the liquid refrigerant (MR-15) is precooled (BPHE-3) and throttled (J-103). Then, it joins the returning streams of the vapor refrigerant (MR-14a and MR-14b). After that, it is divided again into three streams which flow into the precooling BPHEs of the natural gas (BPHE-1), the vapor refrigerant (BPHE-2), and the liquid refrigerant (BPHE-3) respectively to provide the cold capacity. Finally, the three streams converge and flow back to the compressor (C-102).

The advantage of this MSMR process is that the cold capacities of all the refrigerant streams are well utilized. The temperature of the returning MR is higher, which can raise the energy and exergy efficiency of the process. Besides, the natural gas liquid (NGL) recovery system can be integrated between the two BPHEs of the natural gas, namely BPHE-1 and BPHE-4 in Fig. 3(b).

Case 3 is transformed from a MSMR process developed by Pham et al. [27]. The vapor phase of the refrigerant flows back to the compressor directly after providing the cold capacity in the cryogenic heat exchanger instead of flowing back to the precooling heat exchanger. The original process and the process using BPHEs are exhibited in Figs. 4(a) and 4(b), respectively.

In Case 3, the cooling process of natural gas is the same as that in Case 2. The MR is also separated into the vapor phase (MR-2) and the liquid phase (MR-9) before entering the cold box. In this case, the liquid phase is regarded as the heavy part and the vapor phase is regarded as the light part. The heavy part is precooled (BPHE-3), throttled (J-103) and then divided into three streams to provide cold capacity to the three precooling BPHEs (BPHE-1, 2 and 3). The three streams converge afterwards and return to the compressor (C-103). After being pressurized and cooled for the first stage, the stream joins the light refrigerant in MIX-103. The light part is cooled in the precooling and subcooling BPHEs (BPHE-2 and BPHE-5) and then throttled to a lower pressure and temperature. The cold refrigerant is divided into two streams, one going to sub-cool the vapor refrigerant in BPHE-5 and the other to liquefy the natural gas in BPHE-4. The two streams then converge and return to the compressor C-102 directly while the temperature is still far lower than 273 K (220 K–260 K). After being pressurized and cooled for the first stage, the stream joins the heavy refrigerant in MIX-103. Then the MR is separated into the vapor phase (MR-16) and the liquid phase (MR-19). The vapor phase is pressurized and cooled for the second stage while the liquid phase is pumped to the same pressure. They are mixed in MIX-104 and separated again into the vapor phase and the liquid phase. Finally, the two phases return to the cold box as the light part and the heavy part.

The most important feature of Case 3 is that part of the refrigerant returns to the compressor directly at a low temperature instead of going to precooling BPHEs. The decrease in the inlet temperature can massively reduce the power consumption of the compressor so that the energy efficiency of Case 3 can be very high.

Case 4 is the one-separator small-scale offshore BOG re-liquefaction process developed by Nekså et al. [28], which is originally designed with BPHEs. The process includes an MRC and an isolated precooling cycle with propylene. The process is presented in Fig. 5.

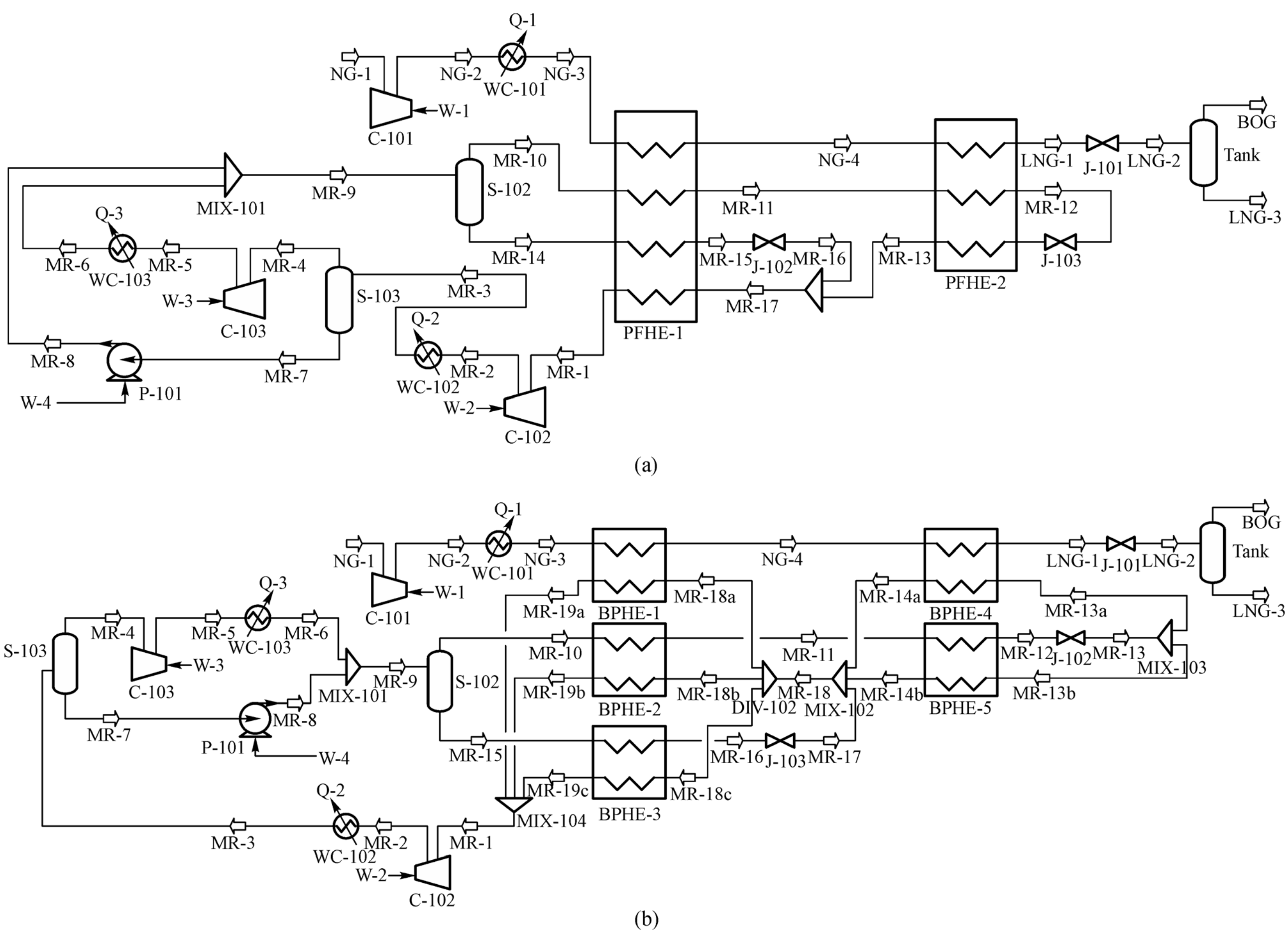

Fig. 3 Original process and modified process using BPHEs.
(a) MSMR process developed by He and Ju (adapted with permission from Ref. [26]; (b) MSMR process using BPHEs (Case 2).

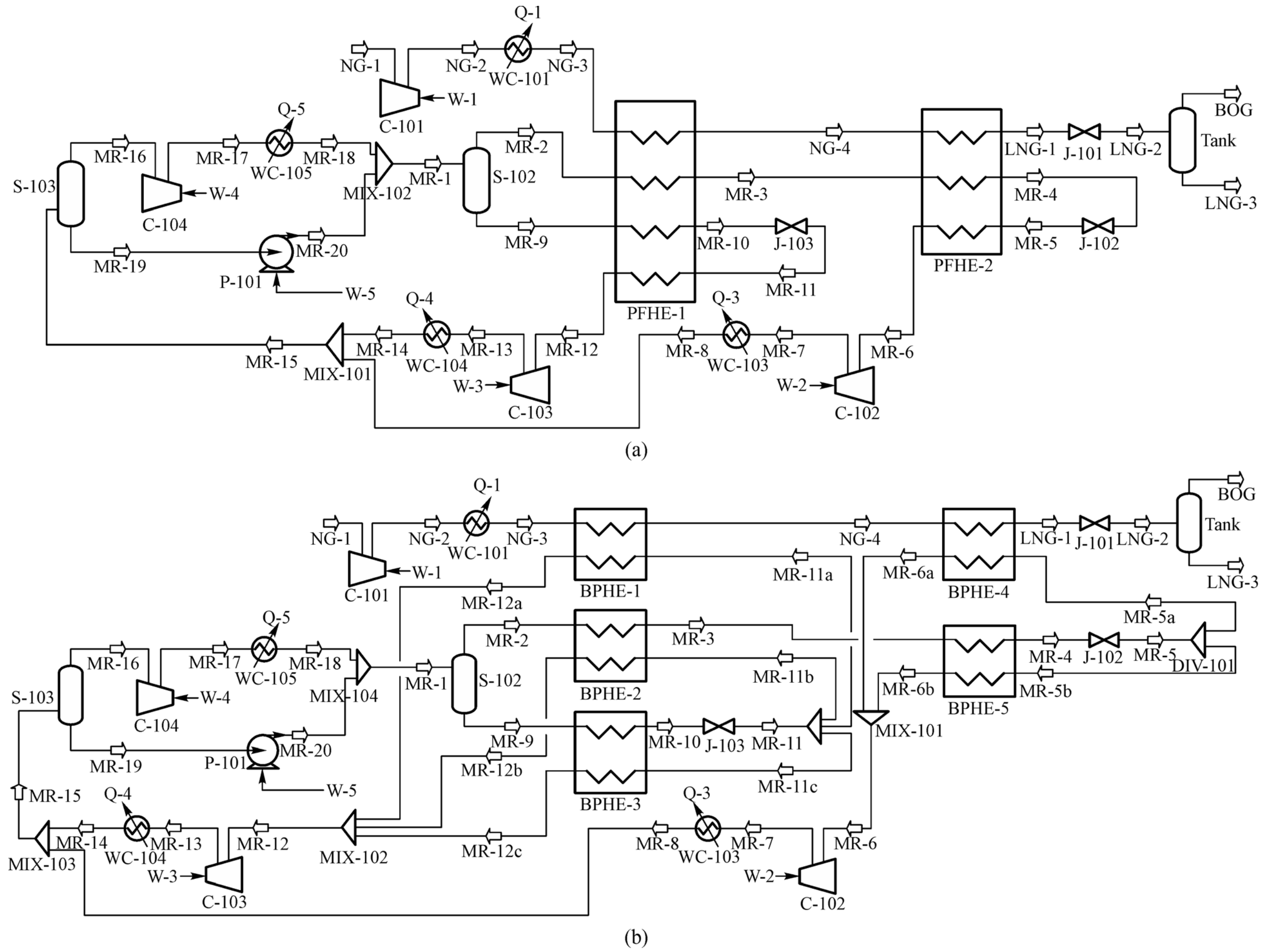

Fig. 4 Original process and process using BPHEs.
(a) MSMR process developed by Pham et al. (adapted with permission from Ref [27]); (b) MSMR process using BPHEs (Case 3).

In Case 4, the cooling process of natural gas is similar to those in Cases 2 and 3. The MR is first pressurized and cooled in two stages (C-102 and C-103). Then, it enters BPHE-3 where it is cooled by the propylene. The precooled natural gas flows into a vapor-liquid separator (S-102). Next, the vapor phase is cooled in the precooling and subcooling BPHE (BPHE-4 and BPHE-5). After that, it is throttled to a lower pressure and temperature and divided into two streams, one of which flows back to the subcooling BPHE (BPHE-5) to liquefy the vapor refrigerant while the other flows to the liquefaction BPHE (BPHE-2) to liquefy the natural gas. The liquid phase is throttled and then directly joins the returning streams of the vapor refrigerant in MIX-102. It flows into the precooling BPHE (BPHE-4) to precool the vapor refrigerant and then returns to the compressor (C-102). The propylene is also pressurized and cooled in two stages (C-104 and C-105). It is throttled through a J-T valve (J-104). After that, the throttled propylene is divided into two streams. They provide cold capacity to the precooling BPHEs of the MR (BPHE-3) and the natural gas (BPHE-1). Finally, the two streams are mixed and return the compressor (C-104).

The advantage of Case 4 is that there are two isolated cycles, which means the process has more optimizable variables so that the optimal operating condition is more likely to be obtained.

The components of the MR are different in the four cases, because they can match better with the structures of the respective processes. Therefore, the components of the MR still refer to the original studies, which are presented in Table 1.

The original processes of the four cases were developed under different conditions. For instance, the composition of the BOG in Case 4 is different from the composition of the natural gas in the other cases. The liquefaction capacities of the cold boxes are also different in the original researches. However, the property and the flow rate of the feed gas of the four cases should be the same in this paper so that the four processes can be compared under a relatively fair condition. Therefore, the flow rate of the

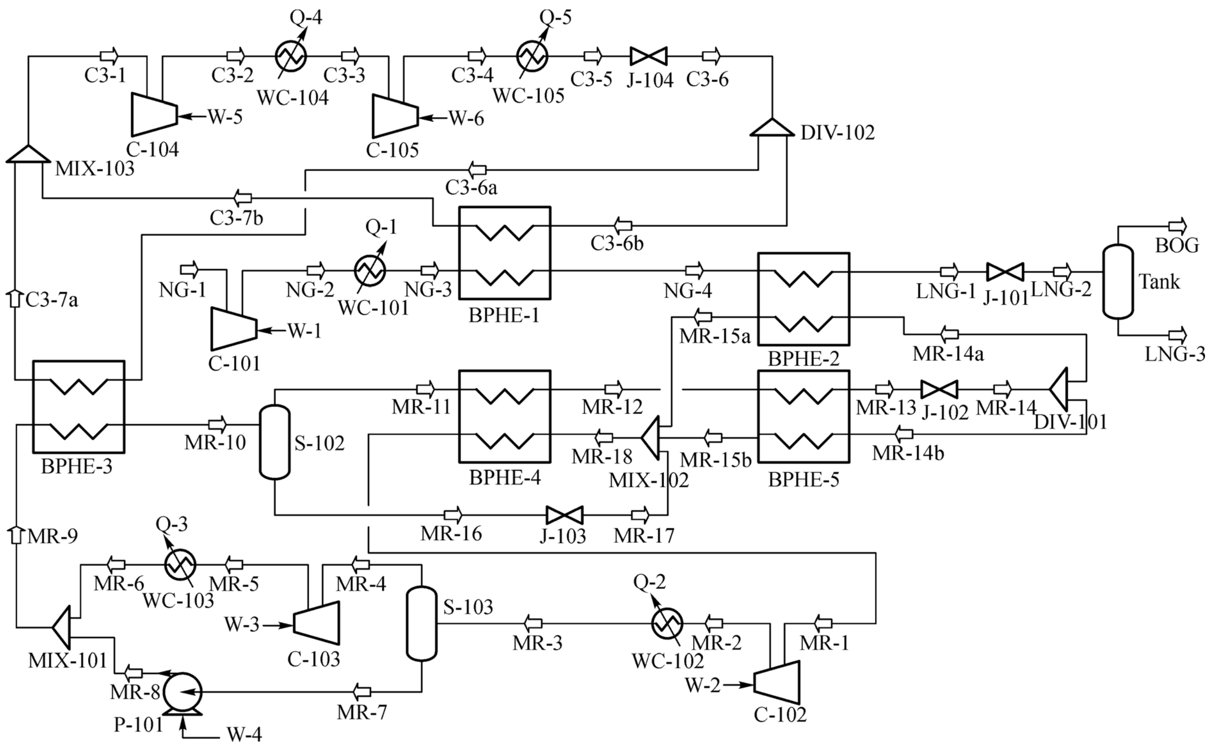

Fig. 5 One-separator small-scale BOG re-liquefaction process (Case 4).

natural gas is assumed as 10000 $N \cdot m^3/d$ in all the cases and the feed gas is defined with the same composition. The variables of the feed gas are presented in Table 2 [27].

Table 1 Components of mixed refrigerant in four cases

Components	Case 1	Case 2	Case 3	Case 4
Methane (CH_4)	√	√	√	√
Ethane (C_2H_6)	√		√	
Propane (C_3H_8)	√		√	√
Iso-butane (i-C_4H_{10})		√		
Nitrogen (N_2)	√	√	√	√
Ethylene (C_2H_4)		√		√

Table 2 Conditions and components of feed gas

Variables	Value
Temperature/K	293
Pressure/kPa	700
Flow rate/($N \cdot m^3 \cdot d^{-1}$)	10000
Methane/(mol%)	93.18
Ethane/(mol%)	5.05
Propane/(mol%)	1.09
I-butane/(mol%)	0.08
N-butane/(mol%)	0.05
Nitrogen/(mol%)	0.55

3 Variable optimization

3.1 Modeling and assumption

Aspen HYSYS, which is widely applied in engineering as a process design and simulation software, is used in this paper to simulate the four cases. The Peng-Robinson equation is selected as the equation of state to calculate the thermodynamic properties, as expressed in Eqs. (1)–(3).

$$P = \frac{RT}{v-b} - \frac{a}{v(v+b)+b(v-b)}, \tag{1}$$

where

$$a = \sum\sum z_i z_j (a_i a_j)^{0.5}(1-k_{ij}), \tag{2}$$

$$b = \sum z_i b_i. \tag{3}$$

All the heat exchangers are calculated based on heat balances and several specifications related to temperatures and enthalpy. In the simulation of all the cases, it is assumed that the adiabatic efficiency of the compressor is 75%. The pressure ratio of each stage is the same if the natural gas or the refrigerant is pressurized in two stages. The minimum temperature approach in each BPHE should be higher than 3 K and there is no heat leakage in all the heat exchangers. The pressure drops in both sides of each BPHE is 10 kPa and there is no pressure drop in the water coolers. The feed gas is pressurized to 4 MPa before entering the cold box in all the cases. Both the feed gas and the refrigerant are cooled to 299 K by the water cooler installed after the compressor. The LNG is subcooled to 113 K in every case in order to reduce the flash gas generated by throttling.

3.2 Description of the optimization method

It is important to compare the cases under their respective optimal conditions. Therefore, the operation variables of all the cases should be optimized. There are many optimizable variables in the LNG processes, all of which can affect the entire process to different extents and the effects of different variables are interrelated. Therefore, a global optimization method is required. The genetic algorithm is selected as the main optimization method in this paper.

The GA, first proposed by Holland [29] in 1975 and widely applied in multivariate optimization by many researchers, is a random search strategy which imitates the biological evolution. In this paper, one set of variables of the LNG process is regarded as an individual. A generation consists of many individuals. The quantity of individuals is the same in each generation, which is regarded as the population. The indicator compared among the cases is defined as the objective function. In general, the energy consumption is a significant criterion to evaluate the LNG process. As a result, the specific energy consumption (SEC) is selected as the objective function in this paper. The SEC is defined as the summation of the power consumed in all the compressors to liquefy the unit flow rate of natural gas, which is given as

$$f(X) = \mathrm{SEC} = \frac{W_{\mathrm{total}}}{\dot{m}_{\mathrm{NG}}}, \tag{4}$$

where X is the optimizable variables, W_{total} is the total power consumption of the compressors and $\dot{m}_{\mathrm{NG}}$ is the flow rate of the natural gas.

The variables in the first generation is randomly generated within a reasonable range, which is selected according to the original value. Then, the objective function of each individual is calculated and compared. Several individuals with the best objective functions are selected. Next, the variables of them cross and new individuals are generated. Most of the individuals in the next generation are generated by crossover while only few are still generated randomly, which are called mutations. Mutation is an effective method to avoid the optimal objective function being trapped at some local optimal points. Then, the second generation repeats the procedure of selection, crossover, mutation and generate a third generation. The algorithm terminates when the number of generations reaches the maximum or the best objective function converges. The framework of the GA is depicted in Fig. 6 and the configuration of the algorithm in this paper is presented in Table 3.

3.3 Penalty function

The best individual can be searched by the algorithm. However, sometimes the variables may cause error in a practical liquefaction system. For instance, the hot and cold composite curves are too close or even cross in a BPHE, or there is liquid in the compressor. Such

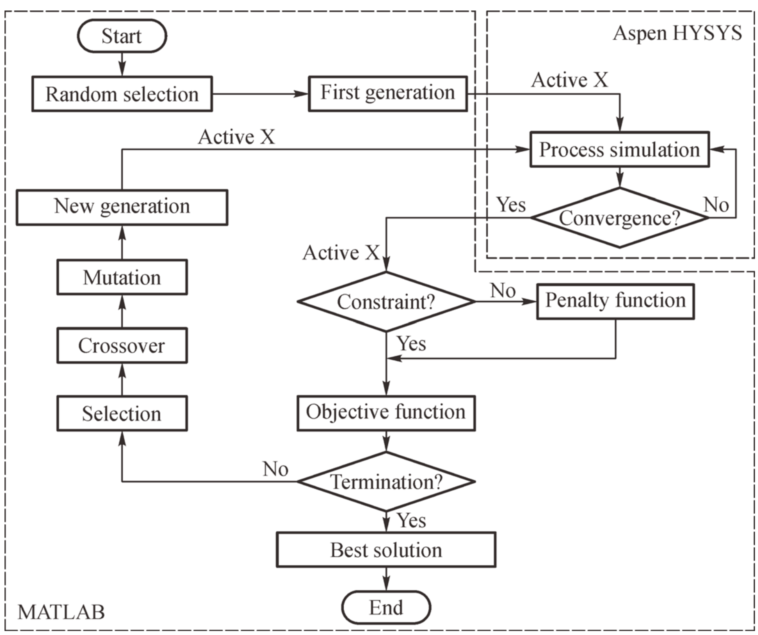

Fig. 6 Flowchart of optimization with GA.

Table 3 Configuration of GA

Population size	Maximum number of generations	Crossover rate	Mutation rate	Selection method	Tournament size
100	200	0.6	0.05	Tournament	4

individuals must be eliminated even if they have better objective functions since these conditions might result in a significant difference between practical engineering and process simulation. When the hot and cold composite curves are too close in the process design, the heat transfer area of the heat exchanger must be very large to meet the heat load requirement, which is unacceptable in the practical cold box. The liquid inside the compressor can cause vibration and noise, and finally do great damage to the equipment. Therefore, the penalty function is defined to enlarge the objective function of such individuals so that the best individuals selected by the algorithm can satisfy all constraints. The penalty function is given in Eqs. (5–7).

$$P(X) = f(X) \cdot e^{g(X)} \cdot e^{h(X)}, \tag{5}$$

$$g(X) = \max(3 - \Delta T_{\min}), \tag{6}$$

$$h(X) = \max(1 - x), \tag{7}$$

where $\Delta T_{\min}$ is the minimum temperature approach of the BPHEs and x is the vapor fraction of the inlet stream of the compressors.

In this paper, the minimum temperature approaches of all the BPHEs are limited to be higher than 3 K so that the hot and cold composite curves do not get too close when turbulence happens in practical engineering application.

4 Results and discussion

The optimizable variables include the pressures after the J-T valves, the MR compressors, and the outlet temperatures of some BPHEs. Besides, the components of the MR also significantly affect the performance of the LNG process. Therefore, the flow rate of each single component is optimized. The numbers of optimizable variables are different in the four cases because the complexities of the processes are different. The decision variables of each case are concluded in Eqs. (8)–(11).

$$X_1 = (\dot{m}_{CH_4}, \dot{m}_{C_2H_6}, \dot{m}_{C_3H_8}, \dot{m}_{N_2}, \mathrm{P}_{MR\text{–}8}, P_{MR\text{–}3}, T_{MR\text{–}4b}, T_{MR\text{–}2}), \tag{8}$$

$$X_2 = (\dot{m}_{CH_4}, \dot{m}_{C_2H_4}, \dot{m}_{i-C_4H_{10}}, \dot{m}_{N_2}, P_{MR\text{–}5}, P_{MR\text{–}13}, P_{MR\text{–}17}, T_{NG\text{–}4}, T_{MR\text{–}11}, T_{MR\text{–}12}, T_{MR\text{–}16}), \tag{9}$$

$$X_3 = (\dot{m}_{CH_4}, \dot{m}_{C_2H_6}, \dot{m}_{C_3H_3}, \dot{m}_{N_2}, P_{MR\text{–}17}, P_{MR\text{–}5}, P_{MR\text{–}11}, T_{NG\text{–}4}, T_{MR\text{–}3}, T_{MR\text{–}4}, T_{MR\text{–}6a}), \tag{10}$$

$$X_4 = (\dot{m}_{CH_4}, \dot{m}_{C_2H_4}, \dot{m}_{C_3H_3}, \dot{m}_{N_2}, \dot{m}_{C_3H_6}, P_{MR\text{–}5}, P_{MR\text{–}14}, P_{C_3\text{–}4}, P_{C_3\text{–}6}, T_{NG\text{–}4}, T_{MR\text{–}10}, T_{MR\text{–}12}, T_{MR\text{–}13}, T_{C_3\text{–}7b}). \tag{11}$$

The ranges for variable searching are given based on the original cases. It should be noted that the ranges are modified because the flow rate of the feed gas has been unified in the present work. The results of the variable optimization are presented in Tables 4–7.

The optimal SECs of the four cases are 0.512, 0.395,

Table 4 Range of variable searching and optimal value in Case 1

Variables	Lower boundary	Upper boundary	Optimal value
$\dot{m}_{CH_4}$ /(N·m^3·d^{-1})	5500	10500	7193
$\dot{m}_{C_2H_6}$ /(N·m^3·d^{-1})	8000	16000	9710
$\dot{m}_{C_3H_8}$ /(N·m^3·d^{-1})	7000	14000	13080
$\dot{m}_{N_2}$ /(N·m^3·d^{-1})	1500	6000	3045
$P_{MR\text{–}8}$/kPa	3000	6000	4807
$P_{MR\text{–}3}$/kPa	160	300	191
$T_{MR\text{–}4b}$/K	283	303	296
$T_{MR\text{–}2}$/K	108	118	113
SEC/(kW·h·(N·m^3)$^{-1}$)			0.512

Table 5 Range of variable searching and optimal value in Case 2

Variables	Lower boundary	Upper boundary	Optimal value
$\dot{m}_{CH_4}$ /(N·m^3·d^{-1})	4000	13500	5608
$\dot{m}_{C_2H_4}$ /(N·m^3·d^{-1})	5500	17000	12510
$\dot{m}_{i-C_4H_{10}}$ /(N·m^3·d^{-1})	8500	12500	9820
$\dot{m}_{N_2}$ / (N·m^3·d^{-1})	1000	4500	2284
$P_{MR\text{–}5}$/kPa	1800	4500	2611
$P_{MR\text{–}13}$/kPa	160	300	232
$P_{MR\text{–}17}$/kPa	160	300	242
$T_{NG\text{–}4}$/K	233	258	251
$T_{MR\text{–}11}$/K	228	243	235
$T_{MR\text{–}12}$/K	108	118	113
$T_{MR\text{–}16}$/K	248	263	256
SEC/(kW·h·(N·m^3)$^{-1}$)			0.395

Table 6 Range of variable searching and optimal value in Case 3

Variables	Lower boundary	Upper boundary	Optimal value
$\dot{m}_{CH_4}/(N\cdot m^3\cdot d^{-1})$	5500	8500	7923
$\dot{m}_{C_2H_6}/(N\cdot m^3\cdot d^{-1})$	6500	11500	10810
$\dot{m}_{C_3H_8}/(N\cdot m^3\cdot d^{-1})$	7000	10500	9317
$\dot{m}_{N_2}/(N\cdot m^3\cdot d^{-1})$	1000	3500	3006
P_{MR-17}/kPa	4000	8000	6405
P_{MR-5}/kPa	160	300	168
P_{MR-11}/kPa	700	1500	1317
T_{NG-4}/K	248	258	253
T_{MR-3}/K	228	243	239
T_{MR-4}/K	103	118	109
T_{MR-6a}/K	223	253	232
$SEC/(kW\cdot h\cdot(N\cdot m^3)^{-1})$			0.383

Table 7 Range of variable searching and optimal value in Case 4

Variables	Lower boundary	Upper boundary	Optimal value
$\dot{m}_{CH_4}/(N\cdot m^3\cdot d^{-1})$	4000	6500	5780
$\dot{m}_{C_2H_4}/(N\cdot m^3\cdot d^{-1})$	12500	15000	13420
$\dot{m}_{C_3H_8}/(N\cdot m^3\cdot d^{-1})$	5500	7500	7305
$\dot{m}_{N_2}/(N\cdot m^3\cdot d^{-1})$	1000	2500	2034
$\dot{m}_{C_3H_6}/(N\cdot m^3\cdot d^{-1})$	14000	18000	15140
P_{MR-5}/kPa	800	2200	1404
P_{MR-14}/kPa	160	300	208
P_{C_3-4}/kPa	800	2200	1243
P_{C_3-6}/kPa	160	300	202
T_{NG-4}/K	243	263	248
T_{MR-10}/K	233	249	246
T_{MR-12}/K	183	203	202
T_{MR-13}/K	108	118	110
T_{C_3-7b}/K	280	288	284
$SEC/(kW\cdot h\cdot(N\cdot m^3)^{-1})$			0.415

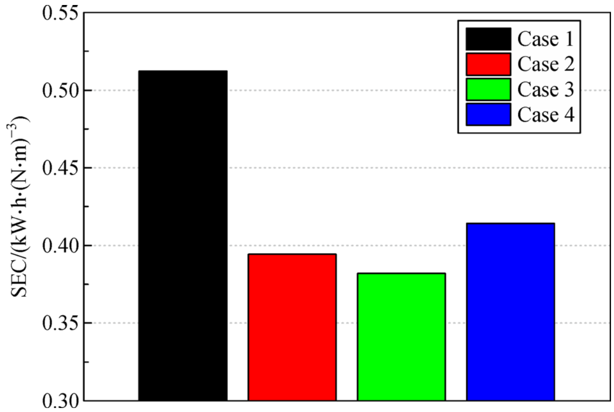

Fig. 7 SECs of optimized cases.

0.383, and 0.415 $kW\cdot h/(N\cdot m^3)$, respectively. It can be concluded from Fig. 7 that Case 3 has the lowest SEC, which is lower by 25.2%, 3.0%, and 7.7% compared with those of Cases 1, 2, and 4. It is mainly due to the special structure of the liquefaction process. In Case 3, part of the refrigerant flows back to the compressor at a very low temperature, which leads to a lower power consumption in the compressor. Another reason is that the composite curves matches better in the BPHEs in Case 3.

The composite curves of the four cases are presented in Fig. 8 and the temperature differences between the feed gas and the refrigerant are compared in Fig. 9. It can be seen in Fig. 8 that the hot and cold composite curves in Case 1 are very close at the cold end and at the liquefaction temperature of the feed gas. However, the shape of the composite curves cannot be adjusted since the entire heat transfer procedure of the feed gas happens only in one BPHE. Because the shapes of the hot and cold composite curves are different, there is a great difference in temperature at the warm end, which obviously declines the heat transfer efficiency. In Case 2, the feed gas is cooled in the two BPHEs, namely the pre-cooling BPHE and the liquefaction BPHE. The refrigerant at the outlet of the liquefaction BPHE does not flow directly into the pre-cooling BPHE. Instead, it is mixed with other refrigerant streams at a higher temperature first and then enters the pre-cooling BPHE. Therefore, the composite curves are much closer at the warm end compared with that in Case 1. Meanwhile, the redundant cold capacity from the liquefaction BPHE is utilized to pre-cool the refrigerant itself, which leads to a high energy efficiency. In Case 3, the refrigerant streams in the pre-cooling BPHE and the liquefaction BPHE are in parallel so that the heat transfer procedure in each of the BPHEs has less influence on the other one, which indicates that the variables can be even more optimizable than that in Case 2. It can be observed in Fig. 9 that the temperature difference at the liquefaction temperature in Case 3 can be as small as that in Case 1 while the temperature difference in the pre-cooling BPHE is much smaller than that in Case 1. Consequently, the SEC of Case 3 is very low. In Case 4, the pre-cooling BPHE and the liquefaction BPHE are in completely different cycles, which is good for the balance of the cold capacity distributed between the two BPHEs. However, as seen in Fig. 8, the composite curves do not match very well at the warm end since the temperature of propylene stays constant when vaporizing. Therefore, the SEC of Case 4 is higher than those of Cases 2 and 3.

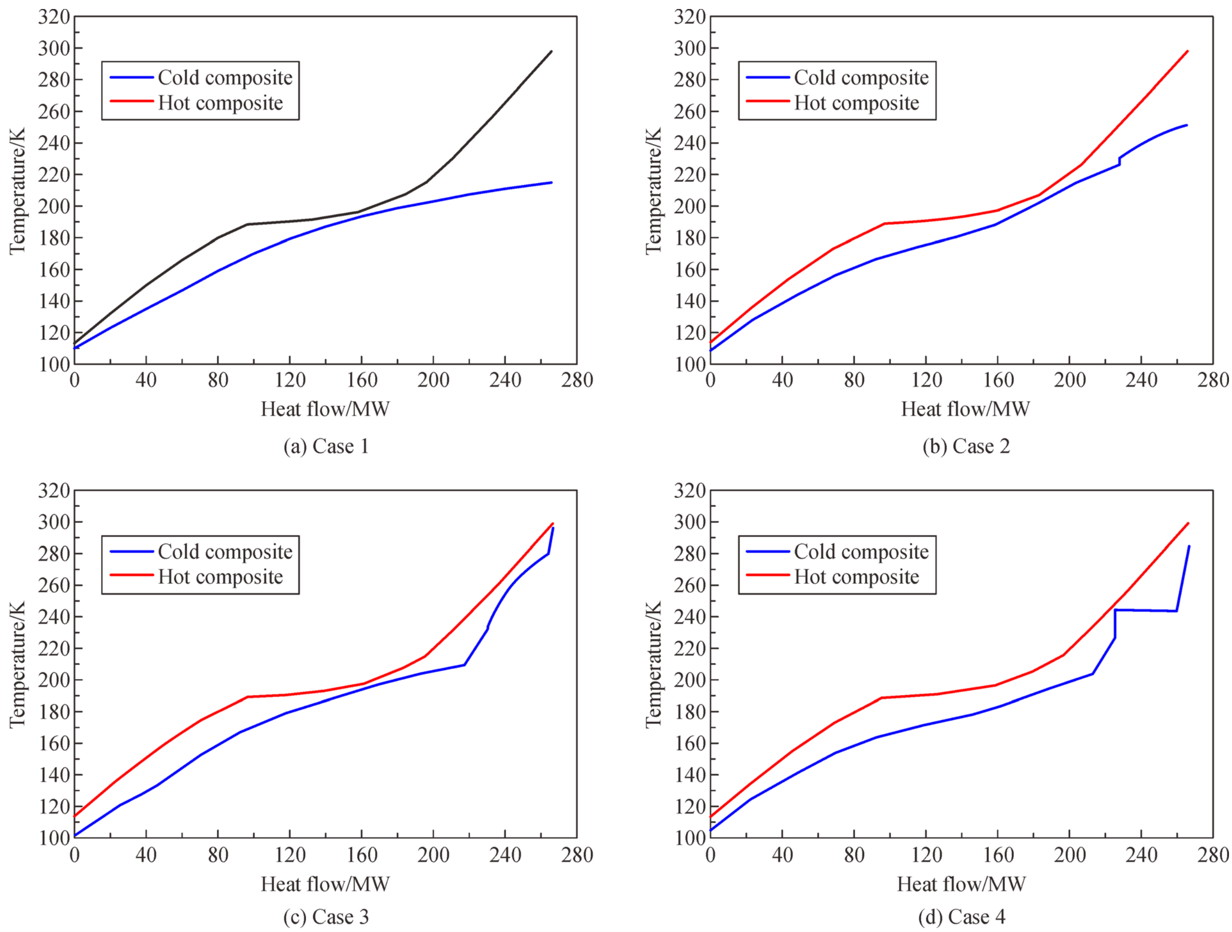

Fig. 8 Composite curves of the four cases.

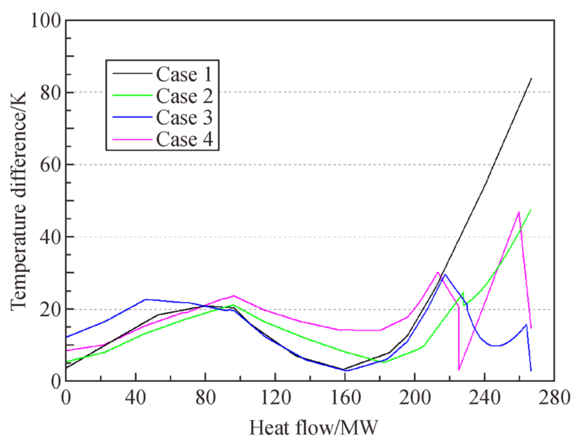

Fig. 9 Comparison of temperature differences between feed gas and refrigerant.

5 Economic analysis

5.1 Economic model

The four cases are compared in terms of economic cost. The total revenue requirement (TRR) method developed by the Electric Power Research Institute [30] is adopted for the economic analysis. Not only the investment of the power consumption and equipment purchase, but also other financial cost derived from the major capital investment such as operation and maintenance costs and equipment depreciation are considered in the TRR method. Therefore, this economic model can give a comprehensive evaluation of the economic performance of the LNG process.

The total revenue requirement is the revenue gained at least from the product of the LNG process to cover the investment. The TRR usually consists of four items, namely return on investment (ROI), fuel cost (FC), operation and maintenance costs (OMC), and total capital recovery (TCR). The total annual revenue requirement in the jth year can be calculated by using Eq. (12).

$$\mathrm{TRR}_j = \mathrm{TCR}_j + \mathrm{ROI}_j + \mathrm{FC}_j + \mathrm{OMG}_j. \qquad (12)$$

The detailed explanation of the economic terms and analysis can be found in Ref. [31]. The economic constants and assumptions are presented in Table 8.

Table 8 Economic constants and assumptions

Economic parameters	Value
Average nominal escalation rate for fuel (r_{FC})/%	5 [32]
Average nominal escalation rate for operating and maintenance cost (r_{OMC})/%	5 [32]
Average annual rate of the cost (i_{eff})/%	10 [32]
Constant cost of electricity consumption (C_e)/(\$·(kW·h)$^{-1}$)	0.071 [8]
Annual operation time (τ)/h	8000 [7]

The PEC of the LNG process can be calculated as the summation of the costs of compressors, heat exchangers, and pumps, since the costs of other equipment such as separators or valves can be neglected compared with them.

$$\mathrm{PEC_{total}} = \mathrm{PEC_{comp}} + \mathrm{PEC_{BPHE}} + \mathrm{PEC_{pump}}. \tag{13}$$

The PEC of compressors depends on the power consumption of the compressors. The equations of the PEC of the compressors are given as follows [33],

$$\mathrm{PEC_{comp}} = 7190 \times W_{\mathrm{comp}}^{0.61}, \tag{14}$$

where W_{comp} is the power consumption of the compressor, hp.

The PEC of BPHEs depends on the heat transfer area, which can be described as the following equation [34],

$$\mathrm{PEC_{BPHE}} = a + bA^n, \tag{15}$$

where a, b, and n are cost constants associated with the type of heat exchanger. For plate heat exchangers, a = 1600, b = 210, and n = 0.95 [33]. A is the heat transfer area of the BPHE, m^2.

The chevron angles of all the BPHEs are assumed as 60°/60°. Thus, the heat transfer coefficient can be calculated by the single-phase or two-phase correlations in BPHE proposed by Khan et al. [35,36]. Then the required heat transfer area can be calculated by using Eq. (16).

$$A = \frac{\Delta h \cdot \dot{m}}{U}, \tag{16}$$

where Δh stands for the absolute value of the change of mass enthalpy through the cold side or the hot side of the BPHE, and U is the total heat transfer coefficient calculated by the correlations.

The PEC of the pumps depends on the flow rate of the fluid that flows through the pump, which can be expressed as [25]

$$\mathrm{PEC_{pump}} = 8000 + 240q^{0.9}, \tag{17}$$

where q is the flow rate of the fluid.

Finally, the levelized total annual revenue requirement $\mathrm{TRR_L}$ within the plant economic time (book life) can be calculated with the capital recovery factor (CRF).

$$\mathrm{TRR_L} = \mathrm{CRE}\sum\nolimits_1^{BL} \frac{\mathrm{TRR}_j}{(1+i_{\mathrm{eff}})^j}, \tag{18}$$

$$\mathrm{CRF} = \frac{1}{\sum\nolimits_1^{BL} \frac{1}{(1+i_{\mathrm{eff}})^j}} = \frac{i_{\mathrm{eff}}(1+i_{\mathrm{eff}})^{BL}}{(1+i_{\mathrm{eff}})^{BL}-1}. \tag{19}$$

5.2 Results and discussion

The PEC of the four cases are illustrated in Table 9 and Fig. 10 which indicate that the PECs of Cases 3 and 4 are high while that of Case 2 is the lowest.

Table 9 PECs of the four cases

Case	$\mathrm{PEC_{comp}}$/\$	$\mathrm{PEC_{BPHE}}$/\$	$\mathrm{PEC_{pump}}$/\$	$\mathrm{PEC_{total}}$/\$
1	278370	8187	8000	294557
2	242350	12130	8000	262480
3	315100	11784	8000	334884
4	305110	12299	8000	325409

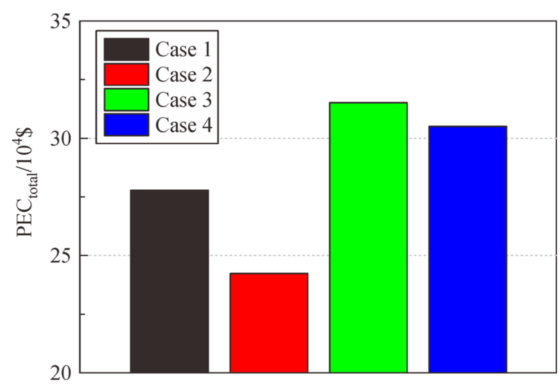

Fig. 10 Total PECs of the four cases.

It can be found in Table 9 that the PECs of the pumps are the same in all cases, because few MR is condensed in the water cooler of the first stage. Thus, the flow rates through the pumps are very low in all the cases. Meanwhile, it is indicated that the PECs of the compressors contribute to the most of the total PEC. There is one more compressor in Case 3 compared with Cases 1 and 2 and there is an extra propylene cycle in Case 4. Consequently, the total PECs of Cases 3 and 4 are much higher. According to the SECs presented in Tables 4 and 5, it can be found that the power consumption of the compressors required in Case 2 is far less than that in Case 1. Therefore, the total PEC of Case 2 is the lowest according to Eq. (14).

The levelized total annual revenue requirement is illustrated in Fig. 11.

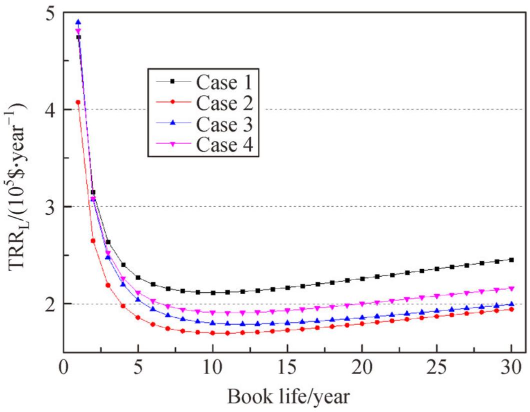

Fig. 11 Levelized total annual revenue requirement of the four cases.

It can be seen in Fig. 11 that the TRR_L decreases apparently when the book life of the LNG plant is less than 5 years but increases slowly when the book life is longer than 10 years. The reason for this is that the PEC of the LNG plant is much higher than the FC and OMC when the book life is very short while the investment of the PEC must be returned within the book life. Therefore, the annual revenue required decreases as the book life lengthens. However, the investments on the FC and OMC should be returned every year while the total PEC does not increase with time. As a result, the TRR_L starts increasing when the book life is long enough as the total FC and OMC exceed the PEC.

It can be also found in Fig. 11 that the TRR_L of Case 3 is the highest when the book life is one year but it soon decreases and becomes lower than those of Cases 1 and 4 when the book life is longer. On the contrary, the TRR_L of Case 1 is the second lowest when the book life is one year, but it becomes the highest when the book life is longer than 2 years. Additionally, the TRR_L of Case 2 is always the lowest when the book life is shorter than 30 years.

The reason for this is that the initial investment of the PEC of Case 1 is very low but the power consumption is the highest of the four cases. Therefore, the disadvantage of the high FC and OMC is increasingly obvious when the book life lengthens. On the contrary, although the PEC of Case 3 is very high, the SEC of Case 3 is much lower than that of the others. Thus, the TRR_L of Case 3 can be advantageous if the book life of the LNG plant is long enough. It is possible that the TRR_L of Case 3 can be even lower than that of Case 2 if the book life is longer than 30 years since it can be seen in Fig. 11 that the blue line is getting closer to the red line with the increment in book life.

In conclusion, the levelized total annual revenue requirement of Case 2 is lower than those of the other three cases when the book life is shorter than 30 years while there is an opportunity that Case 3 is even better if the book life is longer than 30 years. Therefore, the MSMR process with the fully utilization of the cold capacity of the refrigerant (Case 2) and the MSMR process in which part of the refrigerant flows back to the compressor at low temperature (Case 3) are the most economically beneficial LNG processes of the four cases studied in this paper.

6 Robustness evaluation

The condition of gas resource varies within a certain range occasionally in the practical LNG plants, which may influence the performance of the LNG process, or even leads to the failure of equipment sometimes. Consequently, the robustness of the process when disturbance occurs to the gas resource is also of vital importance.

The performance of the LNG process can be apparently influenced by the pressure and flow rate of the feed gas. The increment in flow rate results in closer composite curves in the BPHEs. More heat transfer area is required when the composite curves are too close. The liquefaction ratio of the cold box could be affected if the heat transfer area is not big enough in the BPHEs. On the contrary, if the flow rate of the feed gas decreases, the cold capacity of the refrigerant will be excessive. Thus, the temperature of the refrigerant flowing back to the entrance of the compressor will be lower. It is possible that the refrigerant is not completely vaporized if the temperature is low enough, which will lead to mechanical failures in the refrigerant compressors. Therefore, the LNG process is more reliable in which the temperature of the refrigerant at the inlet of the compressor is much higher than its dew point.

The pressure of the feed gas has obvious influences on the liquefaction temperature and the shape of the hot composite curve. Therefore, the oscillation of the pressure of the feed gas can also affect the performance of the BPHEs.

The four processes are compared with respect to robustness. The maximum allowable ranges of the flow rate and the pressure of the feed gas are obtained based on the optimal operation variables in the LNG process. The constraints are defined as follows: The minimum temperature approaches of all the BPHEs should be higher than 1 K. Besides, there should be no liquid in all the compressors.

The results are shown in Table 10, and Figs. 12 and 13.

As seen from the results, the LNG processes in Cases 1

Table 10 Maximum allowable ranges of pressure and flow rate of feed gas

Case	Maximum pressure of feed gas/kPa	Minimum pressure of feed gas/kPa	Maximum flow rate of feed gas/($N\cdot m^3\cdot d^{-1}$)	Minimum flow rate of feed gas/($N\cdot m^3\cdot d^{-1}$)
1	4340	654	10520	7509
2	25370	617	10364	6226
3	732	653	10093	8861
4	1409	463	10473	8695

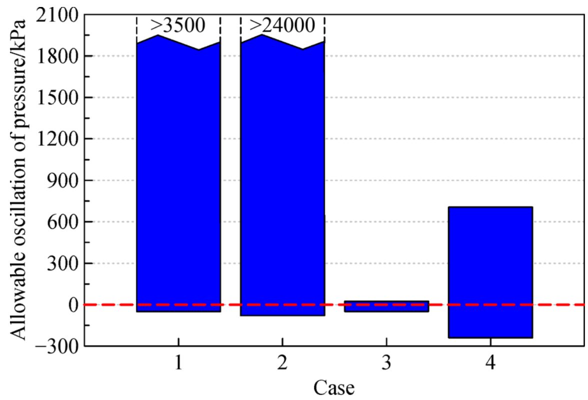

Fig. 12 Maximum allowable range of pressure of feed gas.

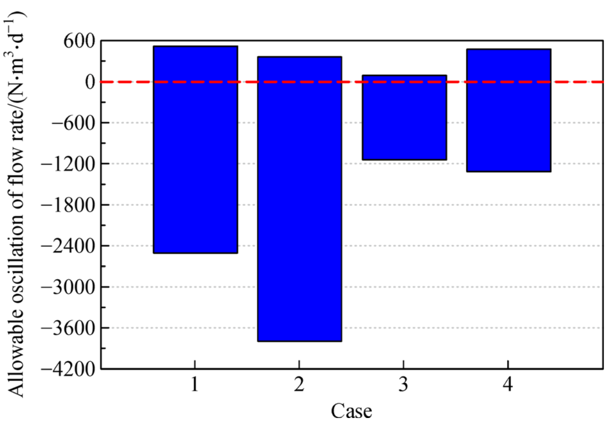

Fig. 13 Maximum allowable range of flow rate of feed gas.

and 2 can still operate under a stable condition when the pressure of the feed gas increases massively or the flow rate of the feed gas decreases greatly. Meanwhile, only the process in Case 4 has a better robustness when the pressure of the feed gas decreases by over 20%. The robustness of the process in Case 3 is apparently worse than that of the others, since the refrigerant in Case 3 flows back to the compressor at a very low temperature while the hot and cold composite curves in the BPHEs are very close under the optimal condition. Consequently, the refrigerant at the inlet of the compressor can be easily liquefied when the flow rate of the feed gas slightly decreases while the temperature approach becomes too close when the flow rate increases or the pressure of the feed gas fluctuates within a small range.

7 Conclusions

In this paper, four different LNG processes using the BPHEs are optimized by using the GA under the same condition of feed gas. The optimal processes are comprehensively compared in terms of energy consumption, economic performance, and robustness. Based on the results, it can be concluded that the MSMR process in which part of the refrigerant flows back to the compressor at low temperature (Case 3) has the lowest power consumption. Meanwhile, the composite curves match the best in Case 3. The SEC of the modified PRICO process (Case 1) is the highest.

The MSMR process in which the cold capacity of the refrigerant is well utilized (Case 2) requires the lowest PEC. The levelized total annual revenue requirement of Case 2 is the lowest when the book life of the LNG plant is shorter than 30 years. There is an opportunity that the levelized total annual revenue requirement of Case 3 can be lower if the book life is longer than 30 years.

Cases 1 and 2 can still operate well when the pressure of the feed gas rises massively or the flow rate of the feed gas decreased greatly. Only the MRC process with a propylene pre-cooling cycle (Case 4) has an ideal robustness when the pressure of the feed gas decreases by over 20%. The robustness of Case 3 is apparently worse than those of the others although the SEC of Case 3 is the best.

It should be noted that there are still some limitations in this paper. Only 4 MRC processes are studied while the performance of the cascade processes and nitrogen expansion processes using BPHEs still needs to be investigated. Moreover, the variable design for the BPHE process is still much stricter than that of the original PFHE process, which may result in a higher SEC. Therefore, the method of transforming the PFHE processes into BPHE processes needs further development to solve this problem.

Notations

A	Heat transfer area/m^2
C_e	Constant cost of electricity consumption/($\$\cdot(kW\cdot h)^{-1}$)
h	Mass enthalpy/($kJ\cdot kg^{-1}$)
m	Flow rate/($N\cdot m^3\cdot d^{-1}$)
P	Pressure/kPa

T	Temperature/K
U	Total heat transfer coefficient/$(\mathrm{kW \cdot (K \cdot m^2)^{-1}})$
W	Power/kW
τ	Annual time of operation/h
BL	Book life
BOG	Boil-off gas
BPHE	Brazed plate heat exchanger
CFD	Computational fluid dynamics
CH_4	Methane
C_2H_4	Ethylene
C_2H_6	Ethane
C_3H_6	Propylene
C_3H_8	Propane
CO_2	Carbon dioxide
COP	Coefficient of performance
CRF	Capital recovery factor
DMR	Dual mixed refrigerant
FC	Fuel cost
FEM	Finite element method
GA	Genetic algorithm
i-C_4H_{10}	Iso-butane
LNG	Liquefied natural gas
MR	Mixed refrigerant
MRC	Mixed refrigerant cycle
MSMR	Modified single mixed refrigerant
N_2	Nitrogen
NGL	Natural gas liquid
OMC	Operation and maintenance costs
PEC	Purchased equipment cost
PFHE	Plate-fin heat exchanger
PNEC	Parallel nitrogen expansion cycle
PRICO	Poly refrigerant integrated cycle operations
ROI	Return on investment
SEC	Specific energy consumption
SMR	Single mixed refrigerant
TCR	Total capital recovery
TRR	Total revenue requirement

References

1. He T, Karimi I A, Ju Y. Review on the design and optimization of natural gas liquefaction processes for onshore and offshore applications. Chemical Engineering Research & Design, 2018, 132: 89–114
2. He T, Chong Z R, Zheng J, Ju Y, Linga P. LNG cold energy utilization: prospects and challenges. Energy, 2019, 170: 557–568
3. Kim D, Hwang C, Gundersen T, Lim Y. Process design and economic optimization of boil-off-gas re-liquefaction systems for LNG carriers. Energy, 2019, 173: 1119–1129
4. Waldrup S P. 2018 Outlook for energy: a view to 2040. ExxonMobil, 2018
5. Nguyen T V, Rothuizen E D, Markussen W B, Elmegaard B. Thermodynamic comparison of three small-scale gas liquefaction systems. Applied Thermal Engineering, 2018, 128: 712–724
6. Khan M S, Lee M. Design optimization of single mixed refrigerant natural gas liquefaction process using the particle swarm paradigm with nonlinear constraints. Energy, 2013, 49: 146–155
7. He T B, Liu Z M, Ju Y L, Parvez A M. A comprehensive optimization and comparison of modified single mixed refrigerant and parallel nitrogen expansion liquefaction process for small-scale mobile LNG plant. Energy, 2019, 167: 1–12
8. Mehrpooya M, Ansarinasab H. Exergoeconomic evaluation of single mixed refrigerant natural gas liquefaction processes. Energy Conversion and Management, 2015, 99: 400–413
9. Qyyum M A, Ali W, Long N V D, Khan M S, Lee M. Energy efficiency enhancement of a single mixed refrigerant LNG process using a novel hydraulic turbine. Energy, 2018, 144: 968–976
10. Tan H B, Shan S Y, Nie Y, Zhao Q X. A new boil-off gas re-liquefaction system for LNG carriers based on dual mixed refrigerant cycle. Cryogenics, 2018, 92: 84–92
11. Cao L, Liu J P, Xu X W. Robustness analysis of the mixed refrigerant composition employed in the single mixed refrigerant (SMR) liquefied natural gas (LNG) process. Applied Thermal Engineering, 2016, 93: 1155–1163
12. Hwang J H, Ku N K, Roh M I, Lee K Y. Optimal design of liquefaction cycles of liquefied natural gas floating, production, storage, and offloading unit considering optimal synthesis. Industrial & Engineering Chemistry Research, 2013, 52(15): 5341–5356
13. Hwang J H, Roh M I, Lee K Y. Determination of the optimal operating conditions of the dual mixed refrigerant cycle for the LNG FPSO topside liquefaction process. Computers & Chemical Engineering, 2013, 49: 25–36
14. Xiong X, Lin W, Gu A. Design and optimization of offshore natural gas liquefaction processes adopting PLNG (pressurized liquefied natural gas) technology. Journal of Natural Gas Science and Engineering, 2016, 30: 379–387
15. de Mello P E B, Villanueva H H S, Scuotto S, Donato G H B, Ortega F D. Heat transfer, pressure drop and structural analysis of a finned plate ceramic heat exchanger. Energy, 2017, 120: 597–607
16. Wang Z, Li Y Z. A combined method for surface selection and layer pattern optimization of a multistream plate-fin heat exchanger. Applied Energy, 2016, 165: 815–827
17. Ma H, Hou C, Yang R, Li C, Ma B, Ren J, Liu Y. The influence of structure parameters on stress of plate-fin structures in LNG heat exchanger. Journal of Natural Gas Science and Engineering, 2016, 34: 85–99
18. Zhan Y, Wang J, Wang W, Wang R S. Dynamic simulation of a single nitrogen expansion cycle for natural gas liquefaction under refrigerant inventory operation. Applied Thermal Engineering, 2018, 128: 747–761
19. Sun H, Hu H, Ding G, Chen H, Zhang Z, Wu C, Wang L. A general distributed-parameter model for thermal performance of cold box with parallel plate-fin heat exchangers based on graph theory.

Applied Thermal Engineering, 2019, 148: 478–490
20. Berstad D, Nekså P, Anantharaman R. Low-temperature CO_2 removal from natural gas. Energy Procedia, 2012, 26: 41–48
21. Wu J T, He T B, Ju Y L. Experimental study on CO_2 frosting and clogging in a brazed plate heat exchanger for natural gas liquefaction process. Cryogenics, 2018, 91: 128–135
22. Wu J T, Ju Y L. Design and optimization of natural gas liquefaction process using brazed plate heat exchangers based on the modified single mixed refrigerant process. Energy, 2019, 186: 115819
23. Aslambakhsh A H, Moosavian M A, Amidpour M, Hosseini M, AmirAfshar S. Global cost optimization of a mini-scale liquefied natural gas plant. Energy, 2018, 148: 1191–1200
24. Lee W, An J, Lee J M, Lim Y. Design of single mixed refrigerant natural gas liquefaction process considering load variation. Chemical Engineering Research & Design, 2018, 139: 89–103
25. Watson H A J, Vikse M, Gundersen T, Barton P I. Optimization of single mixed-refrigerant natural gas liquefaction processes described by nondifferentiable models. Energy, 2018, 150: 860–876
26. He T B, Ju Y L. Design and optimization of a novel mixed refrigerant cycle integrated with NGL recovery process for small-scale LNG plant. Industrial & Engineering Chemistry Research, 2014, 53(13): 5545–5553
27. Pham T N, Khan M S, Minh L Q, Husmil Y A, Bahadori A, Lee S, Lee M. Optimization of modified single mixed refrigerant process of natural gas liquefaction using multivariate Coggin's algorithm combined with process knowledge. Journal of Natural Gas Science and Engineering, 2016, 33: 731–741
28. Nekså P, Brendeng E, Drescher M, Norberg B. Development and analysis of a natural gas reliquefaction plant for small gas carriers. Journal of Natural Gas Science and Engineering, 2010, 2(2–3): 143–149
29. Holland J H. Adaptation in Natural and Artificial Systems: an Introductory Analysis with Applications to Biology, Control and Artificial Intelligence. Cambridge: MIT Press, 1992
30. Technical Assessment Guide (TAGTM). TR-100281 Revision 6 Palo Alto Electric Power Research Institute. CA (Edinburgh), 1993
31. Bejan A TG, Moran M. Thermal Design and Optimization. New York: Wiley, 1996
32. Ghorbani B, Mehrpooya M, Hamedi M H, Amidpour M. Exergoeconomic analysis of integrated natural gas liquids (NGL) and liquefied natural gas (LNG) processes. Applied Thermal Engineering, 2017, 113: 1483–1495
33. CouperJ R, Penney W R, Fair J R. Chemical Process Equipment: Selection and Design. Oxford: Butterworth-Heinemann, 2010
34. Towler Gavin R K S. Chemical Engineering Design: Principles, Practice and Economics of Plant and Process Design. London: Elsevier, 2012
35. Khan T S, Khan M S, Chyu M C, Ayub Z H. Experimental investigation of single phase convective heat transfer coefficient in a corrugated plate heat exchanger for multiple plate configurations. Applied Thermal Engineering, 2010, 30(8–9): 1058–1065
36. Khan T S, Khan M S, Chyu M C, Ayub Z H. Experimental investigation of evaporation heat transfer and pressure drop of ammonia in a 60° Chevron plate heat exchanger. International Journal of Refrigeration, 2012, 35(2): 336–348